A Novel Antioxidant Role for Ligandin Behavior of Glutathione *S*-Transferases: Attenuation of the Photodynamic Effects of Hypericin†

Weiya D. Lu‡ and William M. Atkins*,§

Departments of Chemistry and Medicinal Chemistry, Box 357610, University of Washington, Seattle, Washington 98915-7610

Received April 19, 2004; Revised Manuscript Received July 9, 2004

ABSTRACT: Hypericin (HYP) is a major constituent of the herbal antidepressant St. John's wort with potential utility as an antitumor photodynamic sensitizer and antiviral agent. Upon irradiation at 540−600 nm, HYP generates reactive oxygen species (ROS) and induces oxidative stress. Here, human glutathione *S*-transferase (GST) isoforms GSTP1-1 (P1-1) and GSTA1-1 (A1-1) are shown to bind with high affinity to HYP and to differentially quench its photodynamic properties. In steady-state turnover studies, HYP inhibits A1-1 and P1-1 with IC_{50} values of 160 and 190 nM, respectively. Fluorescence titration experiments and fitting of the data to the Hill equation yield apparent K_Ds for binding to A1-1 and P1-1 of 0.65 and 0.51 μM, respectively. The recovered Hill coefficients are 1.8 for both GSTA1-1 and GSTP1-1, indicating that multiple HYPs bind to each isoform. This behavior is reminiscent of classic "ligandin" activity of GSTs, wherein nonsubstrate planar aromatic anions are sequestered on, and inhibit, the enzyme. However, HYP complexed with P1-1 is photodynamically attenuated, with minimal protein oxidation. In contrast, light-dependent, oxygen-dependent, oxidation of A1-1 was modest and oxidation of human albumin was extensive in the presence of HYP, as monitored by electrospray mass spectrometry (ESI-MS). A peptide "trap" of diffusive ROS was oxidized extensively upon irradiation of HYP in the presence of albumin but very little in the presence of P1-1 or A1-1. Solute quenching studies were used to probe the accessibility of the bound HYP in each of the protein complexes. The fluorescence of HYP complexed with albumin, A1-1, or P1-1 was quenched by I^- with quenching rate constants (k_q) of 1.1×10^9, 2.4×10^9 and 0.5×10^9 M^{-1} s^{-1}, respectively, indicating that small molecules such as O_2 have similar diffusional access to the complexed HYP in each of the proteins, eliminating the possibility of differential accessibility of oxygen as the source of a different yield of ROS. This is the first demonstration of a possible antioxidant role for the ligandin activity of GSTs and a striking example of protein-specific effects on hypericin photodynamic activity. Even highly homologous protein isoforms can differentially promote or inhibit photosensitizer activity.

Photodynamic therapy (PDT)[1] relies on the selective uptake of photosensitizers in tumor cells or associated vasculature, followed by light-dependent production of reactive oxygen species (ROS) and oxidative stress in these tissues (*1*−*3*). Although most sensitizers partition efficiently into organellar membranes, including mitochondrion, in some cases they may also interact with proteins. However, the extent to which individual protein binding sites can modulate the photodynamic properties of various sensitizers has not been studied in detail.

Hypericin (HYP) is a dianthraquinone constituent of St. John's wort, a popular naturopathic herbal remedy for depression (*4*−*6*), and it has long been considered as a potential sensitizer for photodynamic therapy. The molecular mechanism of its anticancer photodynamic properties is not established. Presumably, the cytotoxic effect of HYP results from irradiation with long-wavelength light, producing a high quantum yield of singlet oxygen ($^1O_2$) or other ROS or, possibly, protons. Although the mechanistic details of the resulting cytotoxicity remain unknown, cells irradiated in the presence of HYP experience oxidative stress and apoptosis (*7*, *8*). HYP has been shown also to bind in vitro to protein kinases (*9*), albumin (*10*, *11*), several cytochrome P450 isoforms (*12*), and the steroid X receptor (*13*). HYP may also bind to molten globules (*14*). The structure of HYP is distinct from porphyrin-based PDT agents, such as the prototype hematoporphyrin IX (HPIX) and its analogue verteporfin (Figure 1), but all are hydrophobic planar aromatic compounds.

† This work was supported by the UW NIEHS sponsored Center for Ecogenetics and Environmental Health, Grant NIEHSP30ES07033, and by National Institutes of Health Grants GM62284 and 2 T32 GM008268-16, Training in Molecular Biophysics (W.D.L.).

* Corresponding author. Phone (206) 685-0379. Fax: (206) 685-3252. E-mail: winky@u.washington.edu.

‡ Department of Chemistry, University of Washington.

§ Department of Medicinal Chemistry, University of Washington.

[1] Abbreviations: 4-HNE, 4-hydroxynonenal; CDNB, chloro-2,4-dinitrobenzene; DMSO, dimethyl sulfoxide; ESI-MS, electrospray ionization mass spectrometry; GSH, glutathione; GST, glutathione *S*-transferase; A1-1, GST A class 1-1 dimeric isoenzyme; P1-1, GST P class 1-1 dimeric isoenzyme; HA, human albumin; HPIX, hematoporphyrin IX; HYP, hypericin; MALDI-TOF MS, matrix-assisted laser desorption/ionization−time-of-flight mass spectrometry; PDT, photodynamic therapy; ROS, reactive oxygen species; TCEP, tris(carboxyethyl)phosphine; TFA, trifluoroacetic acid.

10.1021/bi049217m CCC: $27.50
Published on Web 09/14/2004

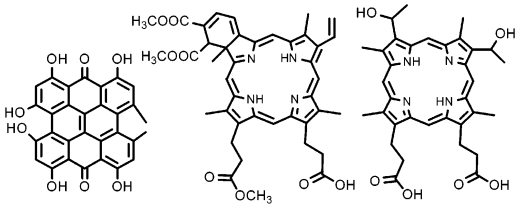

FIGURE 1: Structures of hypericin, used in this work, verteporfin (a clinically used PDT agent), and hematoporphyrin IX (a classic ligandin type inhibitor of GSTs).

On the basis of the molecular structure of HYP, which resembles several known glutathione *S*-transferase (GST) inhibitors (Figure 1), we have explored its interactions with two individual GST isoforms. The GSTs are a canonical family of detoxification enzymes that catalyze the conjugation of the glutathione (GSH) with electrophilic toxins (*15*). GSTs also provide protection from oxidative stress (*16*, *17*). Of particular interest here is the observation that, upon overexpression in model systems, A-class and P-class GSTs confer resistance to oxidative stress (*18*−*20*). It has been suggested that GSTP1-1 directly modulates signal transduction within the Jun/JunK pathway by forming a complex with JunK (*21*−*24*). Furthermore, GSTP1-1 is overexpressed in numerous tumor cell lines and may contribute to drug resistance (*25*). Both A-class and P-class GSTs also directly metabolize lipid peroxides, including those formed during PDT (*17*, *26*), and overexpression of GSTA2-2 or GSTA4-4 has been shown to protect cells from H_2O_2-induced oxidative stress via a direct catalytic clearance of lipid peroxides (*27*). Therefore, cellular expression of GSTs may be a critical determinant of sensitivity to PDT-dependent oxidative stress. Indeed, overexpression of rat GSTA2-2 confers resistance to PDT with rose bengal (*27*).

Interestingly, GSTs also possess a noncatalytic ligand-binding function, wherein they sequester hydrophobic planar aromatic ligands, such as dianthraquinones, at a poorly defined binding site or sites. Binding of steroids, hemes, and other ligands at this GST site(s) may alter their tissue distribution (*28*, *29*). This GST site has been referred to as the "ligandin" site. In fact, a protein originally referred to as ligandin, because of its high affinity for planar aromatic compounds and porphyrins, was subsequently found to be GSTA1-1 (*30*). However, no detoxification role for the ligandin function has been demonstrated. Because GSTs are overexpressed in several tumors that may be candidates for PDT and are implicated in the cellular response to oxidative stress, GST/HYP interactions could lead to interesting and important in vivo effects.

Here, we demonstrate that both GSTA1-1 and GSTP1-1 isoforms bind and are inhibited by HYP with high affinity ($K_D < 0.7\ \mu$M). In addition, the [GST·HYP] complexes yield variable amounts of diffusible ROS compared to free HYP in aqueous solution or complexed to serum albumin. The results provide an interesting example of an antioxidant role for the ligandin function of GSTs, and they set the stage for the possibility of differential responses to HYP in tissues expressing different GSTs. Furthermore, these studies reveal an unanticipated difference in photodynamic properties of a sensitizer bound to structurally homologous proteins of a single family.

MATERIALS AND METHODS

Chemicals and Reagents. Glutathione, chloro-2,4-dinitrobenzene (CDNB), tris(carboxyethyl)phosphine (TCEP), and human albumin (HA) were purchased from Sigma and used without further modifications. Hypericin, ≥99%, from Alexis Biochemicals was verified by mass on a Agilent Technologies LC/MSD series 1100 quadrupole mass spectrometer and used without further modifications. Recombinant human GSTA1-1 (hGSTA1-1) and hGSTP1-1 were expressed as previously described by Ibarra et al. (*31*). Purification of A1-1 was previously described by Ibarra et al. (*32*), and the P1-1 purification is described by Chang and co-workers (*33*) using the glutathione affinity column protocol described by Simons et al. (*34*). TCEP at 1 mM was used to reduce P1-1. The peptide (Genemed Biotechnologies, Inc.) used as a reactive oxygen marker has a monoisotopic molecular mass of 1551.7 Da.

Absorbance/Fluorescence Studies. Absorption spectra were recorded on an upgraded Aminco DW2, On-Line Instrument Systems, Inc. (Olis), using a 10 × 2 mm quartz cuvette (Starna Cells, Atascadero, CA). Protein at 20 μM was mixed with 2 μM HYP in 10 mM potassium phosphate buffer, pH 6.5; these conditions were chosen to reduce the absorbance interference from unbound HYP. Fluorescence ligand-binding and fluorescence quenching studies were performed on an SLM-Aminco 8100 luminometer monitoring hypericin fluorescence with protein titration in a semimicro quartz fluorescence cuvette with excitation along the 10 mm path length. Instrumentation for fluorescence lifetime measurements is described elsewhere (*35*−*37*). HYP solvated in ethanol was used as the stock solution for the protein titration; the total organic content of the final sample solution was <2%. Hypericin fluorescence data were obtained through sample excitation at 549 nm, and the emission spectra were recorded using a long-pass filter at 550 nm (Schott Glass Technologies, Duria, PA). Samples in tryptophan fluorescence studies were excited at 285 nm, and the emission spectra were recorded using a 305 nm (Schott Glass Technologies) long-pass filter. The tryptophan fluorescence was converted to a concentration value by assuming that the fully quenched state was indicative of $[ES] = [E_0]$ and there was a linear relationship between fluorescence quenching and [ES]. The [ES] concentrations were plotted against calculated free ligand concentrations. The binding curves were fitted using Microcal Origin 5.0 software, and dissociation constants were determined using global analysis of multiple experiments at different $[E_0]$ concentrations using the Hill equation for both GSTs:

$$[ES] = \frac{E_0[L]^n}{K_d^n + [L]^n} \quad (1)$$

and a hyperbolic equation for HA:

$$[ES] = \frac{E_0[L]}{K_d + [L]} \quad (2)$$

Solubility of HYP in aqueous solutions has been noted as an experimental concern (*38*). The solubility of HYP was determined to a concentration that encompassed all experi-

mental conditions heretofore. HYP solubility in phosphate buffer, pH 6.5, was determined by visual inspection for absence of particulates and also by absence of optical noise using a Varian Cary 3E spectrophotometer. HYP was found to be soluble up to and including 200 μM.

GST Activity Measurements. Measurements of enzyme activity were based on the formation of a colored conjugate of GSH and CDNB that was monitored at 340 nm. Inhibition studies of 15 nM GSTA1-1 and 33 nM GSTP1-1 in 10 mM potassium phosphate buffer, pH 6.5, were performed at substrate concentrations corresponding to the K_m values of both GSH and CDNB (*33*, *39*) for the respective isoenzyme with varying concentrations of hypericin from a DMSO solvated stock. The final concentration of DMSO did not exceed 5% (v/v). Initial velocities were recorded on a Beckman DU 7400 spectrophotometer.

Whole Protein Oxidation/Mass Spectrometry. The presence of GSH−hypericin conjugates was monitored using MALDI-TOF MS with a Bruker Biflex III and data deconvolution performed by Xmass. For oxidation studies, samples in a dual path length quartz cuvette were illuminated in the 10 mm path length orientation with a 450 W xenon arc lamp passing through a 418 nm long-pass filter (illumination of 418−900 nm) on an SLM-Aminco 8100. Light intensity averaged 4.4 mW/cm^2 (YSI-Kettering model 65 radiometer) from 418 to 650 nm (effective absorption range of hypericin in this system). The samples were irradiated for 0, 10, 30, and 60 min, at which time aliquots were removed for MS analysis. Protein and peptide oxidation were monitored by ESI-MS on a Micromass Quattro II and the mass data deconvoluted by MassLynx. An LC separation with a 50 mm × 2.1 mm POROS R2 column (elution by a linear gradient of a 5%−60% AcCN/0.05% TFA mixture in 7 min at a flow rate of 0.3 mL/min) was used between sample injection and mass analysis as described previously (*39*). Oxidation studies were performed at stoichiometric conditions of 1:1 (GST dimer:ligand), 10 μM GST, and 10 μM hypericin in 10 mM potassium phosphate buffer, pH 6.5. Oxidation studies with HA were performed at 50 μM HA and 50 μM hypericin in phosphate buffer. Due to the lower affinity of hypericin for HA (*38*, *40*), a higher concentration was used to bring the system closer to stoichiometric conditions to mimic those found in the GST·HYP experiments. The peptide concentrations were maintained at 10-fold above the protein concentration. Deoxygenated states were achieved through gentle sparging of samples with argon for 40 min at 4 °C.

GSTA1-1: Tryptic Digestion and Mass Analysis. Samples of GSTA1-1·HYP, both unexposed and exposed to light, were subjected to proteolysis by trypsin (Aldrich). GSTA1-1·HYP at 40 μM in 10 mM potassium phosphate buffer, pH 6.5, after either 0 or 60 min of light exposure (light conditions noted in the preceding paragraph) was diluted with 20 mM ammonium acetate, pH 8.7 (final pH 8.5), and incubated with 1:20 (trypsin:protein complex) equivalents of trypsin for 18 h at 37 °C. Digested fragments were separated by a 100 × 2.0 mm Phenomenex Prodigy Phenyl-3 HPLC column with a Javelin Basic-4 guard column (10 × 2.1 mm) in line with the Micromass mass spectrometer mentioned previously. A gradient of 5%−80% elution solvent B over 30 min was used (solvent A, 0.05% TFA/H_2O, and solvent B, 0.05% TFA/acetonitrile) at a flow rate of 0.3 mL/min.

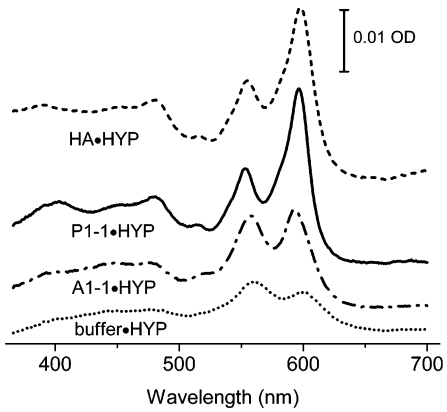

FIGURE 2: Absorption spectra of 2 μM HYP when bound by 20 μM protein in phosphate buffer. Sample conditions from top to bottom, respectively: HA (- - -), P1-1 (—), A1-1 (— · —), and phosphate buffer (· · ·). HYP solvated by protein differs from the unbound HYP in aqueous buffer. The binding site environments are similar for Hyp ligated to P1-1 and HA.

All experimental measurements were acquired with the sample at ambient temperature.

RESULTS

HYP Binding Determined by Fluorescence and Absorbance. The absorption spectrum of HYP bound by GSTA1-1, GSTP1-1, or HA indicates a solubilization of HYP by the three proteins due to the significant spectral difference from HYP in aqueous buffer (Figure 2). The long-wavelength bands at ∼555 and ∼598 nm exhibit inhomogeneous broadening when HYP aggregates in aqueous solution. These bands are sharper in organic solvents or when HYP is solubilized by proteins. The relative intensity of these bands is associated with solvent polarity and aggregated states (*40*, *41*). [P1-1·HYP] and [HA·HYP] have similar spectra and are different from [A1-1·HYP]. Of note, the [HA·HYP] spectrum is similar to those in the literature (*10*, *38*). The spectra of the HYP complexes with P1-1 and HA indicate a hydrophobic binding site and monomeric HYP as suggested by the works of Burel and Jardon (*41*) and Falk and Meyer (*40*, *41*) on HYP homoassociates. Interestingly, given the similarity between the absorbance spectra, i.e., ground state, of HYP bound to GSTP1-1 and HA, one might expect their excited state activities, i.e., photodynamic properties, would also be similar. Upon binding to GSTA1-1 or GSTP1-1, HYP exhibits a very dramatic increase in fluorescence intensity (Figure 3). In fact, in aqueous solution HYP is essentially nonfluorescent due to self-assembly of HYP aggregates (*42*). The increase in fluorescence intensity due to GST binding likely results from the ability of the protein to "dissolve" hydrophobically aggregated HYP. A similar effect has been reported for binding of HYP to a molten globule state of acetylcholinesterase (*14*) and is observed also with albumin (*38*). In addition, titration of GSTA1-1 or GSTP1-1 with HYP resulted in quenching of the intrinsic tryptophan fluorescence, and this provided a convenient method for determination of the binding affinities. For both GSTA1-1 and GSTP1-1, the tryptophan quenching data did not fit well to a standard hyperbolic plot (eq 2). Instead, a Hill plot was required (eq 1, Figure 3 inset) and yielded Hill coefficients, n, of 1.8 ± 0.2 for GSTP1-1 and 1.8 ± 0.2 for GSTA1-1.

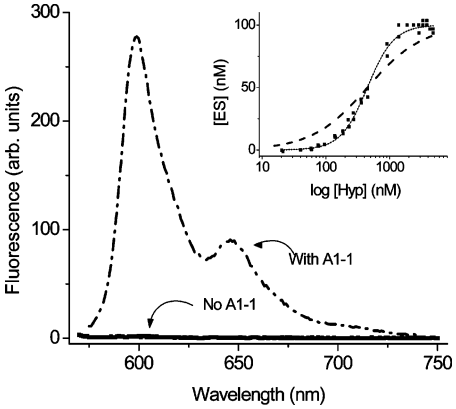

FIGURE 3: Fluorescence spectra of 5 μM hypericin in the absence and presence of 5 μM GSTA1-1, displaying GST-solubilized hypericin via binding, restoring hypericin fluorescence. Inset: Titration of GSTP1-1 (100 nM) intrinsic tryptophan fluorescence with HYP. The solid line is the fit to the Hill equation (eq 2) with a recovered $K_d = 510 \pm 20$ nM and $n = 1.8 \pm 0.2$. The dashed line is the best fit to a hyperbolic binding isotherm, $n = 1$.

This suggests that multiple HYP molecules bind to each GST dimer, with positive cooperativity, but no further mechanistic information is obtained from this analysis. The recovered apparent K_D values are 0.65 ± 0.03 and 0.51 ± 0.02 μM for A1-1 and P1-1, respectively. For reference, the K_D for HYP binding to human albumin is reported to be 1.6 μM (*38*), consistent with our observations ($\sim$1 μM; data not shown). Notably, the binding of HYP to albumin was described well by the standard hyperbolic binding isotherm (eq 1). Also, for comparison, the PDT sensitizer verteporfin was also examined and found to have relatively low affinity ($K_D >$ 80 μM). Therefore, verteporfin was not included in subsequent studies.

Light-Independent Inhibition of GSTs. As an initial characterization of potential interactions between GSTA1-1 or GSTP1-1 and HYP, GST-dependent conjugation of GSH with CDNB was studied at varying concentrations of HYP. Reactions were performed in subdued light to avoid any alterations in GST activity due to HYP-dependent oxidative modification of the enzymes. No GSH conjugates were detected in any incubation, based on MALDI-TOF MS; HYP appears not to be a substrate for A1-1 or P1-1.

However, in the dark, HYP is a very potent reversible inhibitor of both A1-1 and P1-1. Using the standard CDNB assay, at variable concentrations of HYP, the enzymatic activity was decreased in a concentration-dependent fashion, with IC_{50}s of 160 ± 50 nM for A1-1 and 190 ± 6 nM for P1-1, in good agreement with the K_D values based on fluorescence titration. The minor disparity between the apparent K_D values measured by fluorescence titration and the IC_{50} values measured for inhibition of catalytic function is likely due to complex inhibition kinetics, including noncompetitive and competitive components, as observed for hematin, another ligandin substrate (*39*). Regardless of the uncertainty of the inhibition mechanism, these results demonstrate high-affinity interactions between HYP and A1-1 and P1-1. Notably, HYP is a significantly more potent inhibitor than the prototypical ligand inhibitors, such as hematoporphyrin IX, that have K_I values in the range 1−50 μM (*28*, *43*, *44*). Similarly, HYP is a much more potent inhibitor of these GSTs than other proteins, for which HYP-dependent inhibition has been observed. For the majority of proteins suggested to bind HYP, K_D or IC_{50} values in the 1−50 μM range are also observed. In light of the very high expression levels of GSTs in some tissues and their overexpression of GSTs in various tumors, these results suggest the potential for HYP/GST interactions in vivo.

Oxidative Modification of GST by HYP. The observed GST-dependent increase in fluorescence intensity of HYP suggested that monomers of HYP are bound, rather than nonfluorescent HYP aggregates. As a result, we anticipated GST-dependent formation by HYP of reactive oxygen species such as singlet oxygen or other reactive oxygen species. ROS are derived from interaction between molecular oxygen, O_2, and the HYP triplet state, which in turn is generated from the excited, fluorescent, singlet state. Throughout this work, we will refer to the possible oxidizing species as ROS, inasmuch as we have not directly attempted to distinguish between $^1O_2$, hydroxyl radicals, or peroxides. Each of these species may yield oxidized protein. Experiments were done to determine whether the [GST·HYP] complexes yielded ROS upon irradiation.

To characterize the photodynamic behavior of the [GST·sensitizer] complexes, oxidative modification of the proteins was examined by mass spectrometry. HYP was incubated with A1-1, P1-1, or albumin under conditions that minimize free HYP concentration. For HYP, which binds very tightly to both GST isoforms, this was easily accomplished at 10 μM protein and 10 μM HYP. Under these conditions, and based on the experimentally determined apparent K_D, free HYP is 15% of the total, i.e., 1.5 μM. For HYP binding to albumin the expected free concentration is 16%. Notably, the low concentration of free HYP will not contribute to ROS production because of the photodynamic inactivity of HYP aggregates (*41*, *42*). In these in vitro assays, only protein-bound HYP is photodynamically oxidative.

For each protein complex, samples were irradiated for varying times with a high-intensity xenon lamp, before analysis by LC-ESI-MS. A dramatic effect is immediately apparent in the mass spectrum of the GSTA1-1 exposed to light, HYP, and oxygen, the appearance of a manifold of new species with higher masses, in increments of 15−18 amu. With the resolution of these experiments it is reasonable to suggest that these species represent various combinations of singly or multiply oxidized species with incorporation of hydroxyl radical (17 amu), an oxygen atom (16 amu), or peroxyl groups (33 amu), etc. (Figure 4). Given the resolution of the mass spectrometry, it is not possible to unambiguously assign these peaks to specific species and to differentiate between increments of 16−18 mass units. The identity of specific oxidation products is considered in more detail below. Because the protein is not completely oxidized, the presence of this complexity throughout the time course of oxidation suggests that there is not kinetic preference for one peptide to be oxidized. Rather several different peptides may be partially oxidized, resulting in a whole protein mass spectrum with significant heterogeneity. Additionally, other mass increases result from multiple oxidation events in many permutations (*45*) to contribute to a heterogeneous mixture of oxidized products. In essence, the protein is oxidized too extensively to identify all of the discrete products in the mass spectrum. Clearly, however, GSTA1-1 and HA are destroyed upon HYP irradiation concomitant with appearance of the manifold of multiple species of higher mass, and the loss of

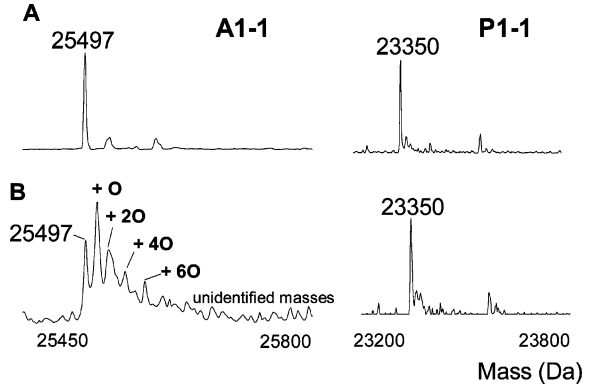

FIGURE 4: ESI-MS spectra of protein oxidation. Spectra are of the GST monomer, and the theoretical masses of A1 and P1 are 25500 and 23350 amu, respectively. Panel A: No illumination of hypericin bound to either A1-1 or P1-1. Panel B: Spectra of GST after 30 min of illumination (see text for conditions). GSTA1-1 yields a distribution of oxidized species at higher molecular weights, of which several has been identified as oxidized products, whereas P1-1 is affected only slightly. In panel B, 10, 20, 30, etc. refer to mass increments of oxygen atoms, or 16, 32, 48, etc., respectively.

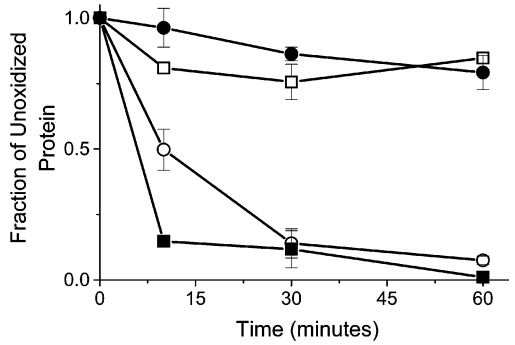

FIGURE 5: Fraction of native protein remaining at various times of light exposure with hypericin bound (see text for conditions). HA is observed to have the fastest rate of degradation/oxidation (■). A1-1 is also oxidized but to a lesser extent (○). P1-1 is oxidized only minimally (●). Protein oxidation requires oxygen, with minimal protein oxidation of A1-1 in the anaerobic state (□). Error bars represent the error for triplicate determination, and in some cases the error bars are smaller than the symbol.

parent ion provides a useful probe of total protein oxidation. We observed a modest light-dependent, HYP-independent, decrease in the parent ion, and all data were corrected for this minor effect (~10%). Interestingly, the extent of oxidation varied significantly with identity of the protein in the order HA > GSTA1-1 ≫ GSTP1-1 (Figure 5). Whereas ~90% of albumin was oxidized in the first 10 min, GSTA1-1 required 30 min to reach a comparable level of oxidation, and GSTP1-1 was highly resistant to oxidation. Apparently, the mode of binding of HYP to GSTP1-1 does not allow for efficient generation of ROS, in marked contrast to HYP bound to albumin and, to a lesser extent, A1-1. To demonstrate that the observed oxidation in the presence of GSTA1-1 was due to the expected mechanisms, reactions were also performed in degassed, partly anaerobic, samples. This nearly eliminated the oxidation for all proteins, with representative results shown for GSTA1-1 (Figure 5, open squares). The loss of parent ion for each protein was clearly dependent on the presence of oxygen.

In addition, we considered the obvious possibility that ROS diffuse from the protein binding sites into bulk solution before oxidizing a different protein molecule. To explore this

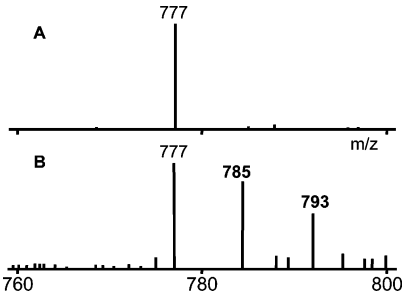

FIGURE 6: Peptide oxidation by light-activated HA-bound hypericin. Panel A: $(M + 2H)^{2+}$ centroid of the native peptide with no illumination. Panel B: The peptide with one (785 mu) and two (793 mu) oxygen atoms incorporated after 60 min of illumination.

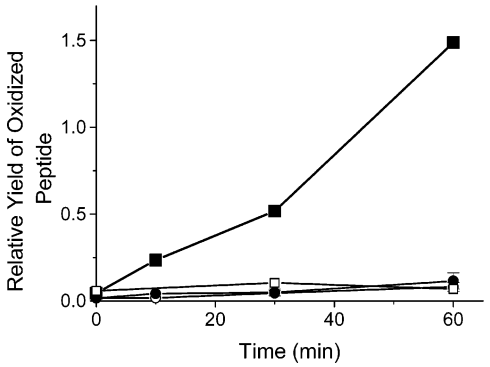

FIGURE 7: Yield of oxygen-adducted peptide relative to non-oxygen-adducted peptide, from 0 to 60 min of light exposure for protein-bound hypericin. Singly and doubly oxygen-adducted peptide peaks were integrated and normalized to the nonoxidized integration. The two oxygen-adducted species were then summed, resulting in a total relative yield of oxidized peptide. There was minimal peptide oxidation with A1-1 (○) and P1-1 (●). Hypericin bound to HA (■) produced ROS that oxidized the peptide. Hypericin bound with A1-1 and P1-1 exhibited ROS production less than the control of hypericin with peptide alone (□). Error bars represent the error for triplicate determination, and in some cases the error bars are smaller than the symbol.

possibility, we exploited a small peptide with no discernible affinity for these proteins that contained an easily oxidizable methionine. Methionine residues are typically the most susceptible to oxidation and are converted to the corresponding sulfoxides and sulfones. The sequence of the peptide used is of no biological significance; it was merely a well-characterized peptide in our laboratory and provided a convenient chemical "trap" for diffusible ROS. This peptide was a useful trap because it contains a single methionine, it has good aqueous solubility and does not bind to or inhibit A1-1 or P1-1, and it has a mass in a convenient range for monitoring discrete oxidation events characterized by mass increases of 16 amu. The sequence is SAEHALTMLNE-HEA.

For this peptide, upon LC-ESI-MS analysis, species with a clear mass increase of 16 and 32 amu were observed, and their formation was dependent on light and oxygen (Figure 6). The concentration of oxidized peptide was monitored as a function of time of irradiation in the absence or presence of each protein and HYP. The greatest oxidation of the peptide occurred in the presence of albumin, for which the peptide was oxidized approximately 1 order of magnitude more rapidly than in the presence of either GST (Figure 7).

To further characterize the oxidation, peptide mapping was performed with the native, unoxidized GSTA1-1 and the

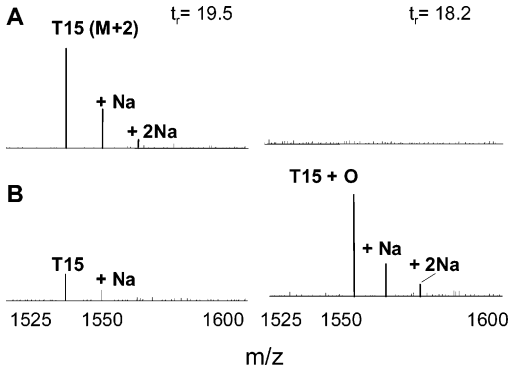

FIGURE 8: ESI-MS spectra of the M + 2 ion of the tryptic peptide T15. The native ion (*m*/*z* 1544) was recovered chromatographically at 19.5 min while the oxidized species (*m*/*z* 1552) eluted at 18.2 min. Loss of the native ion is apparent from no irradiation (panel A, left) to 60 min of irradiation (panel B, left). The oxidized species (+16) was only located in the irradiated sample (panel B, right).

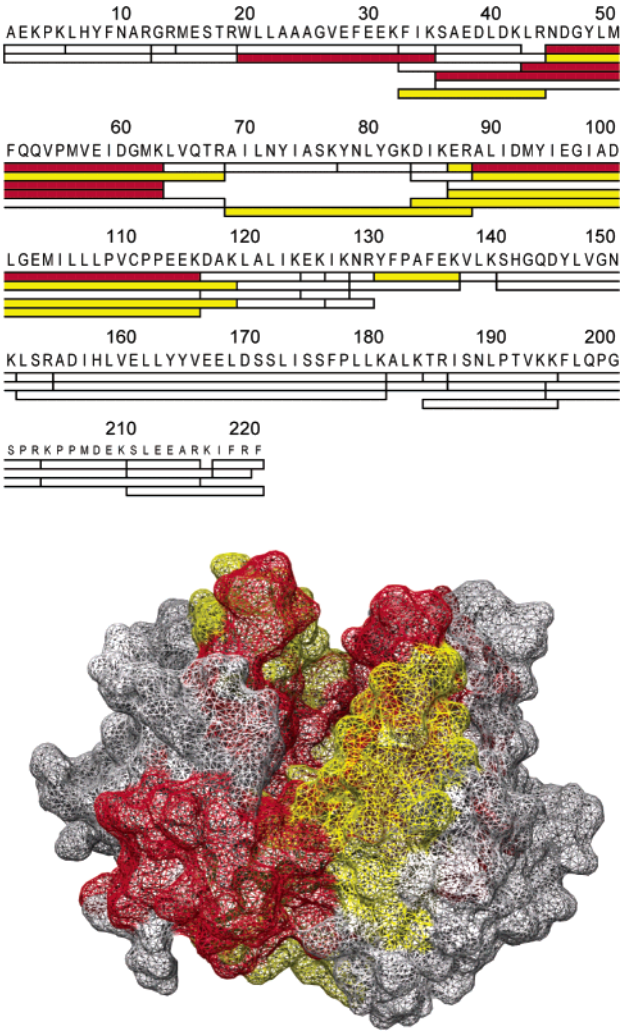

FIGURE 9: Oxidation topography of light-activated GSTA1-1·HYP as illustrated by sequence and surface models. Top panel: The GSTA1-1 primary sequence is shown. Tryptic peptides identified by mass spectrometry are uncolored (100% of sequence). Oxygen-adducted peptides found after 60 min of irradiation are red. Peptides oxidized to unknown products are yellow. Bottom panel: Surface model of GSTA1-1 adapted from PDB file 1GUH (*51*) illustrating the location of the oxidized peptides in the top panel.

partially oxidized protein. GSTA1-1 was digested with trypsin and analyzed by LC-MS. On the basis of the recovered mass of whole peptides from the trypsin-digested GSTA1-1, 100% of the protein sequence was identified. In addition, five peptides, T5-6, T7-9, T8-9, T9, and T15, were observed to decrease with irradiation exposure, and a peptide with corresponding M + 16 and/or higher multiples was observed. The sequences of these peptides are shown in the primary protein sequence in Figure 9. Mass spectra of the native and oxidized T15 peptides are shown in Figure 8. For peptides T9 and T15, the identities of these oxidation products were confirmed by observation of other oxidized peptides that were incompletely cleaved (not shown). These data confirm that oxidation is occurring on the protein.

Interestingly, four of these adducted peptides contain at least one methionine, and the oxidation products are possibly the corresponding sulfoxide. The one peptide exhibiting an oxidation product without a methionine does contain the lone tryptophan, which can form hydroxyl and peroxyl adducts (*45*). The location of these peptides in the three-dimensional folded structure is also shown in Figure 9. In addition, "new" peptides, such as those at *m*/*z* 1103 and 2535 amu, were found to be generated upon oxidation but were not observed in the native protein. The mass of these peptides did not correspond to $(M + n16)^+$, where *n* is an integer, for any peptide, and they remain to be identified. Given the number of reactions that can take place upon exposure to singlet oxygen, including loss of urea from histidine, loss of formyl group from adducted Trp, and cyclization of Tyr and eventual loss of carboxylate (*45*), it is a major challenge to identify each oxidation product. These oxidized peptides with unknown products are depicted in Figure 9 in yellow.

Together, the results clearly indicate that GSTA1-1 is oxidized in a light-, HYP-, and oxygen-dependent manner at several sites within the protein, including some loss of material to unknown products.

Oxygen Accessibility. The combined results of protein oxidation and peptide oxidation indicate significant differences in the yield of ROS with different [protein·HYP] complexes. One obvious possible source of the difference in yield of ROS when HYP is bound to different proteins could be differential accessibility of the excited state of HYP to molecular oxygen. If the binding site on the protein were highly restricted sterically, then O_2 would not have access to the excited state HYP, and no ROS would be generated. Alternatively, a solvent-accessible HYP complex would efficiently yield ROS. As a probe of steric accessibility, therefore, we performed small molecule solute quenching studies. With iodide (I^-), a well-established quencher, the Stern−Volmer quenching constants (K_{SV}) were determined (4.3, 8.3, and 1.9 M^{-1} for GSTA1-1, GSTP1-1, and HA, respectively). In addition, we measured the singlet excited state lifetimes (τ_0) of HYP complexes with A1-1 and P1-1. From K_{SV} and τ_0 the bimolecular rate constant for diffusional quenching by I^- was calculated (Table 1). The important result of these experiments is that albumin, A1-1, and P1-1 yield very similar K_{SV}, τ_0, and k_q values for diffusional quenching of the HYP complexes; in fact, the K_{SV} and k_q are slightly larger for the GSTP1-1 complex. This indicates that differential diffusional accessibility of O_2 to [GSTP1-1·HYP] is not the likely mechanism for the decreased yield of ROS for this complex.

Table 1: Quenching of Hypericin Fluorescence by Iodide[a]

	lifetimes[b] (ps)	K_{SV} (M^{-1})	k_q (10^9 M^{-1} s^{-1})
GSTA1-1·HYP	3800	4.3	1.1
GSTP1-1·HYP	3500	8.3	2.4
HA·HYP	3900[c]	1.9	0.5

[a] Lifetimes of HYP complexed with GSTA1-1 and GSTP1-1 were obtained at 5 μM protein and 0.5 μM HYP in 10 mM phosphate buffer, pH 6.5. Stern−Volmer constants were determined from assay conditions of 10 μM protein and 10 μM HYP in the same buffer, except in the case of albumin where the concentration was 50 μM protein and 50 μM HYP. [b] Weighted-average lifetimes, calculated as $\sum\alpha_i\tau_i$, where α_i and τ_i refer to preexponentials and lifetime of the ith component. [c] Reference *10*.

Table 2: Range of Reactive Oxygen Species Production from the [Protein/Photosensitizer] Interactions of GSTA1-1, GSTP1-1, and Human Albumin[a]

	protein oxidation	diffusing ROS
hypericin in water	−	−
GSTP1-1·HYP	−	−
GSTA1-1·HYP	+	−
human albumin·HYP	++	+

[a] A negative sign (−) indicates negligible or little production, while for those with positive signs, their relative quantities are indicated.

DISCUSSION

St. John's wort is currently an extremely popular herbal antidepressant. A biologically active ingredient of St. John's wort, HYP, also has been used extensively as an antiviral agent and as a sensitizer for PDT. For each of these therapeutic applications, specific cellular targets remain poorly defined. Here we demonstrate that HYP is a very potent inhibitor in vitro of GSTA1-1 and GSTP1-1, and the photodynamic properties of HYP are differentially attenuated when complexed with these proteins. It is difficult to quantitatively determine the yield of ROS in solution, but the protein-dependent attenuation of HYP is qualitatively summarized in Table 2. Importantly, HYP in aqueous solution has little photodynamic activity, because in its aggregated state it is photophysically passivated (*41*). Several independent studies have previously demonstrated that complexation with proteins "activates" HYP in aqueous solution by effectively solubilizing it to its monomeric form (*14*, *38*, *46*). However, no direct comparison within a single study has considered the possibility of differential yield of ROS in different protein environments. The present studies clearly indicate qualitative or quantitative differences in ROS production for [protein·HYP] complexes. Interactions between HYP and these GST isoforms may be particularly relevant for several reasons, as outlined below. First, the specific interactions observed here are discussed.

Dark Reactions. Dark reactions between HYP and GSTs include high-affinity inhibition of GST catalytic activity. This inhibition is not surprising, inasmuch as the ligandin binding sites of GSTs are relatively permissive, and many planar aromatic compounds are nonsubstrate inhibitors. However, the relative affinity of HYP for both GSTA1-1 and GSTP1-1 is significantly greater than most "classic" ligandin-type inhibitors. For comparison, other "ligandin-type" inhibitors exhibit reported K_D values of 0.8−10 μM (*28*, *43*, *44*). Due to the relatively high affinity of GST·HYP binding and instrumental sensitivity limits, we encountered significant challenges in attempting to determine true K_Ds. The apparent K_Ds reported here are almost certainly upper limits, because they were performed at protein concentrations nearly equal to the apparent K_D. The combination of a very high level expression of GSTs in several tumor cells and normal tissues and high affinity binding suggests the possibility that HYP uptake by cells could be affected by GST expression. Indeed, it has been suggested that cellular uptake and localization of hematoporphyrin and indocyanine dyes are altered by expression of, and binding to, GSTs (*47*−*49*).

Light Reactions. The combination of high affinity for GSTs along with their high level expression may also have implications for the photodynamic processes of HYP in some cell types. Light-dependent reactions between HYP and albumin or GSTs include oxidation of the protein and oxidation of small molecules in solution. Although the results demonstrate that the ROS yield of HYP is attenuated when bound to GSTs compared to albumin, they do not afford a detailed mechanism for this effect. Several possible mechanisms may be operative, including decreased population of the first excited singlet state, decreased intersystem crossing to the triplet state, or decreased triplet state lifetime. On the basis of the dramatic increase in fluorescence of HYP upon binding to GSTA1-1 or GSTP1-1, which occurs from the first excited singlet state, it is unlikely that the first mechanism is relevant. Furthermore, the difference in absorbance spectra of HYP complexed with the different proteins does not correlate with the oxidative potency, and this amplifies the fact that ground state difference alone cannot account for differences in ROS production. It would be interesting to determine how the triplet state properties are altered upon GST binding, but this will require additional studies.

A striking observation of the protein oxidation studies is the significant difference between the sensitivity of GSTA1-1 vs GSTP1-1 to oxidation. This observation provides a strong example of protein-dependent photodynamic behavior of a bound sensitizer, even for closely related isoforms within a canonical family. Such a protein dependence does not appear to be widely appreciated in the literature. The solute quenching studies indicate that this difference is not due to differential accessibility of HYP to oxygen, to the extent that I^- has diffusional properties similar to O_2; oxygen does not appear to be sterically excluded from HYP complexed to GSTP1-1 any more than HYP complexed to GSTA1-1 or albumin. We propose that even subtle differences in the HYP binding sites are sufficient to alter that excited state processes that determine the yield of ROS, as already noted in Table 2.

Possible GST/HYP Interactions. Like other PDT sensitizers, HYP induces oxidative stress. In contrast, A-class GSTs and GSTP1-1 confer protection against oxidative stress via their catalytic and regulatory activities, which lead to metabolism of lipid peroxides and modulation of JunK, respectively. Specifically, A-class GSTs metabolize lipid peroxides and 4-hydroxynonenal (4-HNE) (*50*) and contribute to antioxidative stress responses via catalytic activities that are inhibited by ligandin-type inhibitors such as HYP.

Based on the results, it is interesting to speculate that overexpression of GSTP1-1 would be expected to decrease the efficacy of HYP, which is photodynamically quenched

upon complexation. Notably, photodynamic therapy in model systems has been successful even in cells that express GSTs. To our knowledge a direct comparison of HYP sensitivity between cells with different GST expression has not been made. However, it is conceivable that the dose−response curve is adversely shifted when GST is overexpressed, and the magnitude of this effect would depend on the GST isoform. Such speculation obviously requires further study, but the current results reveal that the HYP oxidative potential is differentially modulated by complexation with different proteins, *including* structurally homologous members of a single canonical family (29% sequence identity, calculated by the SIB BLAST network). In cases where complexation occurs with sufficiently high affinity to highly expressed proteins, this could increase or decrease the photodynamic efficacy of sensitizers: protein binding, and possibly GST binding, could be a confounding variable of PDT. Moreover, the results provide an interesting new example of a potential antioxidant role for GSTs via their ligandin function, which contrasts the previously established antioxidant roles for the catalytic activity and signal transduction properties. Interestingly, GST-dependent sequestration by itself would not detoxify photosensitzers, but sequestration combined with photodynamic passivation could alleviate oxidative stress. Similar effects for ligandin activity may be envisioned with endogenous prooxidants such as bilirubin or biliverdin, although their affinities for GSTs are lower than the HYP example.

ACKNOWLEDGMENT

We thank Dr. Theo Bammler of the University of Washington Department of Environmental Health for providing the recombinant hGSTP1-1 cell line and Professor Jake Petrich and Dr. Pramit Chowdhury of Iowa State University for assistance in obtaining fluorescence lifetimes for HYP complexed with GSTA1-1 and P1-1. Additionally, we thank Dr. Claudia Jochheim for invaluable assistance with mass spectral analysis. Molecular graphics images were produced using the UCSF Chimera package from the Computer Graphics Laboratory, University of California, San Francisco (supported by NIH Grant P41 RR-01081).

REFERENCES

1. Foote, C. S. (1987) Type-I and Type-II Mechanisms of Photodynamic-Action, *ACS Symp. Ser. 339*, 22−38.
2. Girotti, A. W. (1990) Photodynamic lipid peroxidation in biological systems, *Photochem. Photobiol. 51*, 497−509.
3. Ahmad, N., and Mukhtar, H. (2000) Mechanism of photodynamic therapy-induced cell death, in *Singlet Oxygen, Uv-a, and Ozone 319*, 342−358.
4. Barnes, J., Anderson, L. A., and Phillipson, J. D. (2001) St. John's wort (*Hypericum perforatum* L.): a review of its chemistry, pharmacology and clinical properties, *J. Pharm. Pharmacol. 53*, 583−600.
5. Bennett, D. A., Jr., Phun, L., Polk, J. F., Voglino, S. A., Zlotnik, V., and Raffa, R. B. (1998) Neuropharmacology of St. John's Wort (*Hypericum*), *Ann. Pharmacother. 32*, 1201−1208.
6. Ernst, E. (1999) Second thoughts about safety of St. John's wort, *Lancet 354*, 2014−2016.
7. Assefa, Z., Vantieghem, A., Declercq, W., Vandenabeele, P., Vandenheede, J. R., Merlevede, W., de Witte, P., and Agostinis, P. (1999) The activation of the c-Jun N-terminal kinase and p38 mitogen-activated protein kinase signaling pathways protects HeLa cells from apoptosis following photodynamic therapy with hypericin, *J. Biol. Chem. 274*, 8788−8796.
8. Agostinis, P., Assefa, Z., Vantieghem, A., Vandenheede, J. R., Merlevede, W., and De Witte, P. (2000) Apoptotic and anti-apoptotic signaling pathways induced by photodynamic therapy with hypericin, *Adv. Enzyme Regul. 40*, 157−182.
9. de Witte, P., Agostinis, P., Van Lint, J., Merlevede, W., and Vandenheede, J. R. (1993) Inhibition of epidermal growth factor receptor tyrosine kinase activity by hypericin, *Biochem. Pharmacol. 46*, 1929−1936.
10. Das, K., Smirnov, A. V., Wen, J., Miskovsky, P., and Petrich, J. W. (1999) Photophysics of hypericin and hypocrellin A in complex with subcellular components: Interactions with human serum albumin, *Photochem. Photobiol. 69*, 633−645.
11. Das, K., Smirnov, A. V., Wen, J., Miskovsky, P., and Petrich, J. W. (1999) Photophysics of hypericin and hypocrellin A in complex with subcellular components: interactions with human serum albumin, *Photochem. Photobiol. 69*, 633−645.
12. Obach, R. S. (2000) Inhibition of human cytochrome P450 enzymes by constituents of St. John's Wort, an herbal preparation used in the treatment of depression, *J. Pharmacol. Exp. Ther. 294*, 88−95.
13. Wentworth, J. M., Agostini, M., Love, J., Schwabe, J. W., and Chatterjee, V. K. (2000) St. John's wort, a herbal antidepressant, activates the steroid X receptor, *J. Endocrinol. 166*, R11−R16.
14. Weiner, L., Roth, E., Mazur, Y., and Silman, I. (1999) Targeted cross-linking of a molten globule form of acetylcholinesterase by the virucidal agent hypericin, *Biochemistry 38*, 11401−11405.
15. Xue, L., He, J., and Oleinick, N. L. (1999) Promotion of photodynamic therapy-induced apoptosis by stress kinases, *Cell Death Differ. 6*, 855−864.
16. Baez, S., Segura-Aguilar, J., Widersten, M., Johansson, A. S., and Mannervik, B. (1997) Glutathione transferases catalyse the detoxication of oxidized metabolites (o-quinones) of catecholamines and may serve as an antioxidant system preventing degenerative cellular processes, *Biochem. J. 324* (Part 1), 25−28.
17. Berhane, K., Widersten, M., Engstrom, A., Kozarich, J. W., and Mannervik, B. (1994) Detoxication of base propenals and other alpha, beta-unsaturated aldehyde products of radical reactions and lipid peroxidation by human glutathione transferases, *Proc. Natl. Acad. Sci. U.S.A. 91*, 1480−1484.
18. Klotz, L. O., Fritsch, C., Briviba, K., Tsacmacidis, N., Schliess, F., and Sies, H. (1998) Activation of JNK and p38 but not ERK MAP kinases in human skin cells by 5-aminolevulinate-photodynamic therapy, *Cancer Res. 58*, 4297−4300.
19. Luna, M. C., Wong, S., and Gomer, C. J. (1994) Photodynamic therapy mediated induction of early response genes, *Cancer Res. 54*, 1374−1380.
20. Tao, J., Sanghera, J. S., Pelech, S. L., Wong, G., and Levy, J. G. (1996) Stimulation of stress-activated protein kinase and p38 HOG1 kinase in murine keratinocytes following photodynamic therapy with benzoporphyrin derivative, *J. Biol. Chem. 271*, 27107−27115.
21. Yang, Y., Cheng, J. Z., Singhal, S. S., Saini, M., Pandya, U., Awasthi, S., and Awasthi, Y. C. (2001) Role of glutathione S-transferases in protection against lipid peroxidation. Overexpression of hGSTA2-2 in K562 cells protects against hydrogen peroxide-induced apoptosis and inhibits JNK and caspase 3 activation, *J. Biol. Chem. 276*, 19220−19230.
22. Xie, C., Lovell, M. A., Xiong, S., Kindy, M. S., Guo, J., Xie, J., Amaranth, V., Montine, T. J., and Markesbery, W. R. (2001) Expression of glutathione-S-transferase isozyme in the SY5Y neuroblastoma cell line increases resistance to oxidative stress, *Free Radical Biol. Med. 31*, 73−81.
23. Wang, T., Arifoglu, P., Ronai, Z., and Tew, K. D. (2001) Glutathione S-transferase P1-1 (GSTP1-1) inhibits c-Jun N-terminal kinase (JNK1) signaling through interaction with the C terminus, *J. Biol. Chem. 276*, 20999−21003.
24. Adler, V., Yin, Z., Fuchs, S. Y., Benezra, M., Rosario, L., Tew, K. D., Pincus, M. R., Sardana, M., Henderson, C. J., Wolf, C. R., Davis, R. J., and Ronai, Z. (1999) Regulation of JNK signaling by GSTp, *EMBO J. 18*, 1321−1334.
25. Tew, K. D., Monks, A., Barone, L., Rosser, D., Akerman, G., Montali, J. A., Wheatley, J. B., and Schmidt, D. E., Jr. (1996) Glutathione-associated enzymes in the human cell lines of the National Cancer Institute Drug Screening Program, *Mol. Pharmacol. 50*, 149−159.
26. Hayes, J. D., and Pulford, D. J. (1995) The glutathione S-transferase supergene family: regulation of GST and the contribution of the isoenzymes to cancer chemoprotection and drug resistance, *Crit. Rev. Biochem. Mol. Biol. 30*, 445−600.

27. Lavoie, L., Tremblay, A., and Mirault, M. E. (1992) Distinct oxidoresistance phenotype of human T47D cells transfected by rat glutathione S-transferase Yc expression vectors, *J. Biol. Chem. 267*, 3632−3636.
28. Smith, A., Nuiry, I., and Awasthi, Y. C. (1985) Interactions with glutathione S-transferases of porphyrins used in photodynamic therapy and naturally occurring porphyrins, *Biochem. J. 229*, 823−831.
29. Listowsky, I., Abramovitz, M., Homma, H., and Niitsu, Y. (1988) Intracellular binding and transport of hormones and xenobiotics by glutathione-S-transferases, *Drug Metab. Rev. 19*, 305−318.
30. Habig, W. H., Pabst, M. J., Fleischner, G., Gatmaitan, Z., Arias, I. M., and Jakoby, W. B. (1974) The identity of glutathione S-transferase B with ligandin, a major binding protein of liver, *Proc. Natl. Acad. Sci. U.S.A. 71*, 3879−3882.
31. Ibarra, C., Grillo, M. P., Lo Bello, M., Nucettelli, M., Bammler, T. K., and Atkins, W. M. (2003) Exploration of in vitro pro-drug activation and futile cycling by glutathione S-transferases: thiol ester hydrolysis and inhibitor maturation, *Arch. Biochem. Biophys. 414*, 303−311.
32. Ibarra, C., Nieslanik, B. S., and Atkins, W. M. (2001) Contribution of aromatic−aromatic interactions to the anomalous p*K*(a) of tyrosine-9 and the C-terminal dynamics of glutathione S-transferase A1-1, *Biochemistry 40*, 10614−10624.
33. Chang, M., Bolton, J. L., and Blond, S. Y. (1999) Expression and purification of hexahistidine-tagged human glutathione S-transferase P1-1 in *Escherichia coli*, *Protein Expression Purif. 17*, 443−448.
34. Simons, P. C., and Vander Jagt, D. L. (1977) Purification of glutathione S-transferases from human liver by glutathione-affinity chromatography, *Anal. Biochem. 82*, 334−341.
35. Gai, F., Fehr, M. J., and Petrich, J. W. (1993) Ultrafast excited-state processes in the antiviral agent hypericin, *J. Am. Chem. Soc. 115*, 3384−3385.
36. Gai, F., Fehr, M. J., and Petrich, J. W. (1994) Role of solvent in excited-state proton-transfer in hypericin, *J. Phys. Chem. 98*, 8352−8358.
37. Gai, F., Fehr, M. J., and Petrich, J. W. (1994) Observation of excited-state tautomerization in the antiviral agent hypericin and identification of its fluorescent species. *J. Phys. Chem. 98*, 5784−5795.
38. Senthil, V., Longworth, J. W., Ghiron, C. A., and Grossweiner, L. I. (1992) Photosensitization of aqueous model systems by hypericin,. *Biochim. Biophys. Acta 1115*, 192−200.
39. Lyon, R. P., and Atkins, W. M. (2002) Kinetic characterization of native and cysteine 112-modified glutathione S-transferase A1-1: reassessment of nonsubstrate ligand binding, *Biochemistry 41*, 10920−10927.
40. Falk, H., and Meyer, J. (1994) On the homo-association and heteroassociation of hypericin, *Monatsh. Chem. 125*, 753−762.
41. Burel, L., and Jardon, P. (1996) Homo-association of hypericin in water and consequences on its photodynamic properties. *J. Chim. Phys. Phys.-Chim. Biol. 93*, 300−316.
42. Darmanyan, A. P., Burel, L., Eloy, D., and Jardon, P. (1994) Singlet oxygen production by hypericin in various solvents, *J. Chim. Phys. Phys.-Chim. Biol. 91*, 1774−1785.
43. Tipping, E., Ketterer, B., and Koskelo, P. (1978) The binding of porphyrins by ligandin, *Biochem. J. 169*, 509−516.
44. Shichi, H., and O'Meara, P. D. (1986) Purification and properties of anionic glutathione S-transferase from bovine ciliary body, *Biochem. J. 237*, 365−371.
45. Davies, M. J. (2003) Singlet oxygen-mediated damage to proteins and its consequences, *Biochem. Biophys. Res. Commun. 305*, 761−770.
46. Hadjur, C., Jeunet, A., and Jardon, P. (1994) Photosensitization by hypericin−Electron-spin-resonance (Esr) evidence for the formation of singlet oxygen and superoxide anion-radicals in an in-vitro model, *J. Photochem. Photobiol., B 26*, 67−74.
47. Thomas, R. S., Gustafson, D. L., Ramsdell, H. S., el-Masri, H. A., Benjamin, S. A., and Yang, R. S. (1998) Enhanced regional expression of glutathione S-transferase P1-1 with colocalized AP-1 and CYP 1A2 induction in chlorobenzene-induced porphyria, *Toxicol. Appl. Pharmacol. 150*, 22−31.
48. Sugimoto, M., Shimada, N., Aikawa, K., and Sugiyama, Y. (1993) Relationship between content of hepatic glutathione S-transferases and the kinetics of indocyanine green elimination in various liver diseases, *Biopharm. Drug Dispos. 14*, 567−578.
49. Abels, C., Fickweiler, S., Weiderer, P., Baumler, W., Hofstadter, F., Landthaler, M., and Szeimies, R. M. (2000) Indocyanine green (ICG) and laser irradiation induce photooxidation, *Arch. Dermatol. Res. 292*, 404−411.
50. Nanduri, B., Hayden, J. B., Awasthi, Y. C., and Zimniak, P. (1996) Amino acid residue 104 in an alpha-class glutathione S-transferase is essential for the high selectivity and specificity of the enzyme for 4-hydroxynonenal, *Arch. Biochem. Biophys. 335*, 305−310.
51. Sinning, I., Kleywegt, G. J., Cowan, S. W., Reinemer, P., Dirr, H. W., Huber, R., Gilliland, G. L., Armstrong, R. N., Ji, X., Board, P. G., et al. (1993) Structure determination and refinement of human alpha class glutathione transferase A1-1, and a comparison with the Mu and Pi class enzymes, *J. Mol. Biol. 232*, 192−212.

BI049217M